BRL MR 2709

BRL

MEMORANDUM REPORT NO. 2709

CONTROL DYNAMICS OF HUMAN TRACKING WITH A VISCOUSLY DAMPED TRACKING AID

Robert T. Gschwind

December 1976

USA BALLISTIC RESEARCH LABORATORIES
ABERDEEN PROVING GROUND, MARYLAND

Destroy this report when it is no longer needed.
Do not return it to the originator.

Secondary distribution of this report by originating or sponsoring activity is prohibited.

Additional copies of this report may be obtained from the National Technical Information Service, U.S. Department of Commerce, Springfield, Virginia 22151.

The findings in this report are not to be construed as an official Department of the Army position, unless so designated by other authorized documents.

UNCLASSIFIED

SECURITY CLASSIFICATION OF THIS PAGE *(When Data Entered)*

REPORT DOCUMENTATION PAGE		READ INSTRUCTIONS BEFORE COMPLETING FORM
1. REPORT NUMBER BRL MEMORANDUM REPORT NO. 2709	2. GOVT ACCESSION NO.	3. RECIPIENT'S CATALOG NUMBER
4. TITLE *(and Subtitle)* CONTROL DYNAMICS OF HUMAN TRACKING WITH A VISCOUSLY DAMPED TRACKING AID		5. TYPE OF REPORT & PERIOD COVERED Final 6. PERFORMING ORG. REPORT NUMBER
7. AUTHOR(s) Robert T. Gschwind		8. CONTRACT OR GRANT NUMBER(s)
9. PERFORMING ORGANIZATION NAME AND ADDRESS US Army Ballistic Research Laboratory Aberdeen Proving Ground, MD 21005		10. PROGRAM ELEMENT, PROJECT, TASK AREA & WORK UNIT NUMBERS RDTE Project 1W662618AH80
11. CONTROLLING OFFICE NAME AND ADDRESS US Army Materiel Development and Readiness Command 5001 Eisenhower Avenue Alexandria, VA 22333		12. REPORT DATE DECEMBER 1976 13. NUMBER OF PAGES 28
14. MONITORING AGENCY NAME & ADDRESS *(if different from Controlling Office)*		15. SECURITY CLASS. *(of this report)* UNCLASSIFIED 15a. DECLASSIFICATION/DOWNGRADING SCHEDULE

16. DISTRIBUTION STATEMENT *(of this Report)*

Approved for public release; distribution unlimited.

17. DISTRIBUTION STATEMENT *(of the abstract entered in Block 20, if different from Report)*

18. SUPPLEMENTARY NOTES

19. KEY WORDS *(Continue on reverse side if necessary and identify by block number)*

Viscous damping
Tracking aids
Human tracking
Control theory
Human transfer function

20. ABSTRACT *(Continue on reverse side if necessary and identify by block number)* (bjk)

This report presents an analysis of viscously damped tracking aids. It applies classical control theory to the problem. It supports the argument with a series of simulations with a human in the loop. It gives some preliminary design guidance for stiffness and damping. Finally, it discusses some general applications and requirements for future research.

DD FORM 1 JAN 73 1473 EDITION OF 1 NOV 65 IS OBSOLETE

UNCLASSIFIED

SECURITY CLASSIFICATION OF THIS PAGE *(When Data Entered)*

TABLE OF CONTENTS

I. INTRODUCTION

This report presents an analysis of viscously damped tracking aids. The problem begins when a human needs to manually point something like a weapon or a camera. The pointing accuracy can be improved if the object is supported by something like a tripod and if viscous damping is added to smooth out the tracking. This report applies classical control theory to the problem. It supports the argument with a series of simulations with a human in the loop. It gives some preliminary design guidance for stiffness and damping. Finally, it discusses some general applications and requirements for future research.

Viscously damped tracking aids have been used since 1962. At that time the US Army Human Engineering Laboratories started using them for directing anti-tank guided missiles.[1,2,3] Currently there are approximately four Army applications and at least one commercial camera tripod that use viscous damping. They have been designed with the general notion that there should be a lot of damping so as to mask the effect of inertia; that the legs should be as stiff as possible to prevent windup and oscillations; and that the coulomb friction should be as low as possible. The amount of inertia has always been a fixed parameter determined by the device being pointed. Several iterations of build and test have achieved very fine performance indeed. For example, a nominal set of specifications might be as follows:

Inertia	$J = 1$ slug-ft^2
Damping	$B = 100$ ft-lb/rad/sec
Stiffness	$K = 10000$ ft-lb/rad
Accuracy	RMS = 100 microrad (low tracking rates)

Until now no one has performed the classical-control analysis to make determinations of design parameters.

II. SYSTEM MODEL

The first step was to develop a model of the control loop. The lumped parameter model, block diagram, and transfer functions shown in

---

[1] R. T. Gschwind, "Gunner Tracking Behavior as a Function of Three Different Control Systems," Human Engineering Laboratories Technical Memorandum 2-63, January 1963. AD-404 055

[2] R. T. Gschwind, "Gunners' Aiming Errors in Antitank Weapons," Human Engineering Laboratories Technical Memorandum 5-64, Feb 64. AD-351 392

[3] F. N. Newcomb, "Viscous-Damping Mechanisms as Applied to 4-Inch Rocket Launcher Mount," Human Engineering Laboratories Technical Note, Feb 63. AD-403 672

Figure 1 are the result of the following rationale and simplifying assumptions:

a. It is a one-dimensional tracker.

b. The human applies torque directly to the load through a fixed handle; therefore, there is no gear reduction or backlash.

c. All inertia, J, is located in the rotating mass.

d. All compliance, K_T, is located between the damper and the ground.

e. The viscous damping, B, is linear with angular rate.

f. There is no coulomb friction.

g. An optical sight provides a visual error signal to the human representing the angular error between the device angle, and the reference (target) location, r.

h. The sight provides enough magnification that the eyeball threshold is not reached.

i. Whatever the sight magnification is, it is included in the human gain K_H.

j. The human output torque is linear with respect to error regardless of magnitude.

A human transfer function was chosen from "Man-Machine System" by Sheridan and Ferrell. Actually, Sheridan selected it. He believed for a simple task such as a heavily damped tripod with a low frequency reference task that a pure lag, $\tau = 0.3$ seconds, and a gain, K_H, would be a good approximation of a human; furthermore, the Padé Approximation can be used for such a low frequency problem.

$$Y_H = K_H \exp(-\tau s) \simeq K_H (1 - \frac{\tau}{2} S)/(1 + \frac{\tau}{2} S)$$

The transfer function resulting from these assumptions is shown in Figure 1. It was used in the several analyses that follow.

III. ROUTH STABILITY CRITERION

Routh Stability Criterion was applied to the characteristic equation to find the upper bound on human gain, K_H, as a function of the tripod parameters J, K_T, and B. This analysis presumes that the human

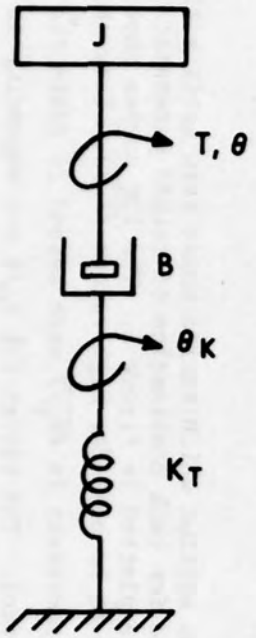

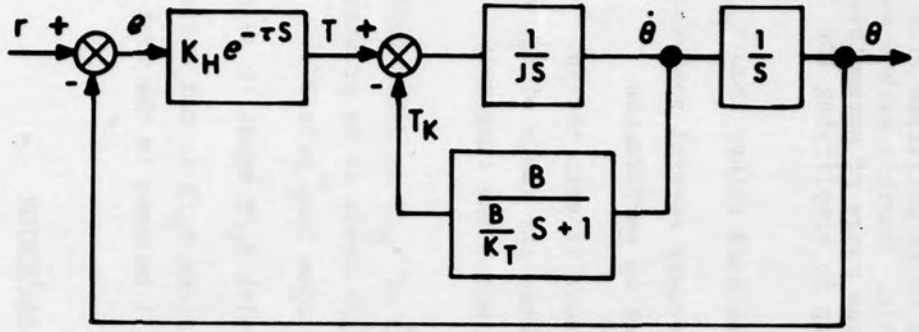

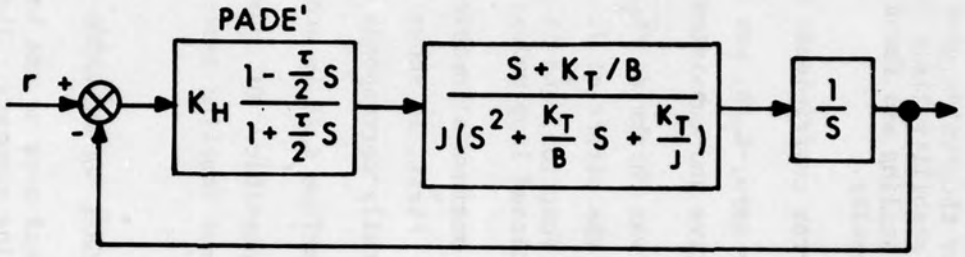

$$J\ddot{\theta} = T - T_K$$

$$\dot{T}_K = K_T(\dot{\theta} - \dot{\theta}_B)$$

$$B\dot{\theta}_B = T_K$$

$$\dot{\theta}_B = \dot{\theta} - \dot{\theta}_K$$

$$F_{OL} = \frac{K_H(6.6 - S)(S + \frac{K_T}{B})}{JS(6.6 + S)(S^2 + \frac{K_T}{B}S + \frac{K_T}{J})}$$

Figure 1. Physical Model and Block Diagram

can increase his gain almost without limit until he is satisfied with the system performance or the system goes unstable. Routh's method was an easy way to find the stability limit for a wide range of parametric values. Actually, some scaling was found to help in simplifying the presentation of these results.

a. The velocity error coefficient, K_H/B, was used rather than K_H.

b. The closed loop zero, $-K_T/B$, was used because several analyses show it to have a sensitive and consistent effect on performance.

c. The final term was chosen as $\sqrt{K_T/J}$ because it gets the job done; i.e., it includes the effect of J, it reduces the range of K_T, it appears in the transfer function, and it approximates the imaginary dimension of a pair of closed loop poles.

Figure 2 shows the maximum allowable values of K_H/B as determined from Routh's Criterion. First, it shows that K_T/B needs to be greater than 6.6, which incidentally corresponds to the open loop pole $-2/\tau$. Second, it shows that maximum K_H/B is achieved with K_T/B equal to 14 and with $\sqrt{K_T/J}$ as large as possible. Of course, maximum K_H/B is not necessarily the same as minimum tracking error as will be seen in the next two analyses.

IV. INTEGRAL SQUARE-ERROR (ISE) CRITERION

The ISE Criterion was used to see how the choice of system parameter values can affect tracking accuracy. The ISE was selected because it can be calculated from the transfer function, thereby permitting easy variation of parameter values. The solution of the integral can be found in Analytical Design of Linear Feedback Systems, by Newton, 1957. For convenience the computational algorithm is presented on a separate page (Table I).

A FORTRAN program was written which varied human gain until a minimum value of ISE was found for each combination of tripod parameter values. These results are plotted in Figure 3. The ISE curves show a ratio of K_T/B equal to 10 to be best for high values $\sqrt{K_T/J}$. They show diminishing benefits for increases in $\sqrt{K_T/J}$ much beyond 25 (note the ordinate does not go to zero). The values for K_H/B corresponding to minimum ISE are not shown; however, a value of 3.0 was near optimum for nearly all of the better combinations.

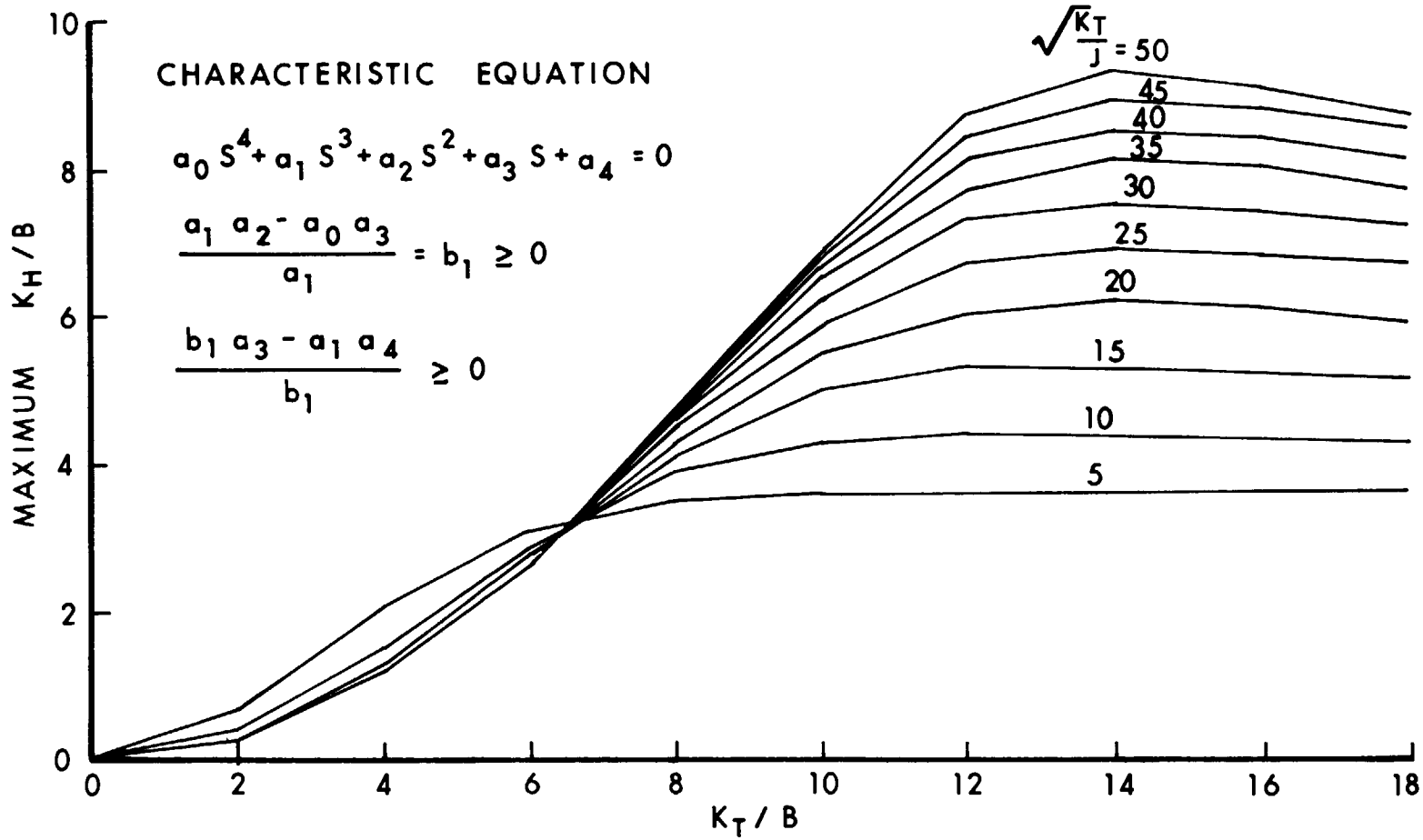

Figure 2. Routh's Stability Criteria

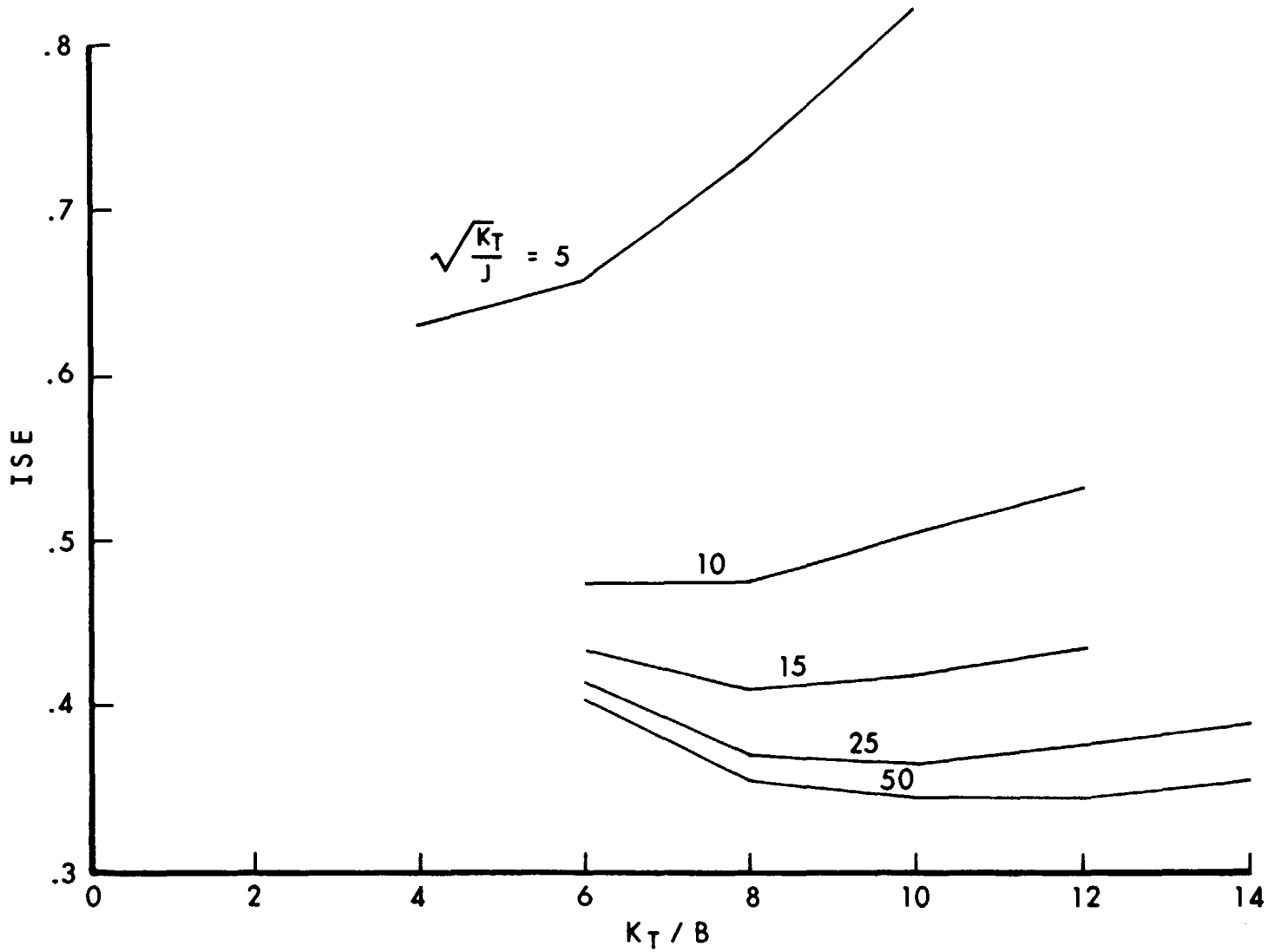

Figure 3. ISE

TABLE I. ISE Computational Algorithm

$$ISE = \int_0^{\infty} e^2(t)dt = \frac{1}{2\pi j}\int_{-\infty}^{+\infty} \frac{C(s)C(-s)}{D(s)D(-s)}\, ds$$

where $e(t)$ = error as a function of time

$C(s)/D(s)$ = frequency domain representation of $e(t)$.

$$C(s) = c_o + c_1 s + c_2 s^2 + c_3 s^3$$

$$D(s) = d_o + d_1 s + d_2 s^2 + d_3 s^3 + d_4 s^4$$

$$c_o = K_T$$

$$c_1 = (J/B + \tau/2)\ K_T$$

$$c_2 = (1 + \tau/2 \cdot K_T/B)J$$

$$c_3 = J \cdot \tau/2$$

$$d_o = K_H K_T/B$$

$$d_1 = K_T + K_H - K_H(K_T/B)\tau/2)$$

$$d_2 = (J\ K_T/B + K_T\tau/2 - K_H\tau/2)$$

$$d_3 = c_2$$

$$d_4 = c_3$$

$$ISE = \frac{\left\{c_3^2\ (-d_o^2 d_3 + d_o d_1 d_2) + (c_2^2 - 2c_1c_3)\ d_o d_1 d_4 + (c_1^2 - 2c_o c_2)\ d_o d_3 d_4 + c_o^2(-d_1 d_4^2 + d_4 d_3 d_2)\right\}}{\left\{2d_o d_4\ (-d_o d_3^2 - d_1^2 d_4 + d_1 d_2 d_3)\right\}}$$

The ISE is not a very selective measure of performance as compared to the ITAE considered next. These results do, however, give a good general picture of how performance is affected by the parameter variations, and they give a good starting point for the ITAE analysis, namely:

$K_T/B = 10$

$\sqrt{K_T/J} = 30$

$K_H/B = 3.0$

V. INTEGRAL-OF-TIME-MULTIPLIED ABSOLUTE ERROR (ITAE) CRITERION

The ITAE Criterion is more selective than the ISE. It will select a system that damps out faster than the ISE because it multiplies the error by time. The bad feature of the ITAE is that it must be determined by measurement of the system response unlike the ISE and Routh's Criterion which may be calculated from the transfer function. The ITAE was determined from the closed loop response to a unit step as calculated by DYSYS, a Fourth Order Runge-Kutta Routine. A calculation was made every tenth second for four seconds after the step. The absolute error was multiplied by time and by the time increment and summed up to get the ITAE. Figure 4 shows two step-responses which indicate that the four-second duration approached infinity for purposes of this problem.

The scaled parameters were varied one at a time until a minimum ITAE was achieved. This minimum value was used while another parameter was varied until a new minimum was found, and so on. The data collected during this procedure are listed in Table II. Many of these data are plotted in Figure 5. The bottom curve shows the ITAE to be very selective in that there is a clearly defined minimum at K_T/B equal to eight. Further changes in the other two parameters could produce no more reduction. There is always the possibility that the coarseness of this analysis could overlook the true minimum, but for now the ITAE Criterion indicates an optimum design:

$K_T/B = 8.0$

$\sqrt{K_T/J} = 30$

Remember that this optimum is for a step input and a particular human transfer function. Additional support and verification are required before concluding it is the optimum design.

VI. ROOT LOCUS METHOD

Root locus plots help to understand why the tripod legs should have some compliance and why there is an optimum value of K_T/B. Figure 6 was

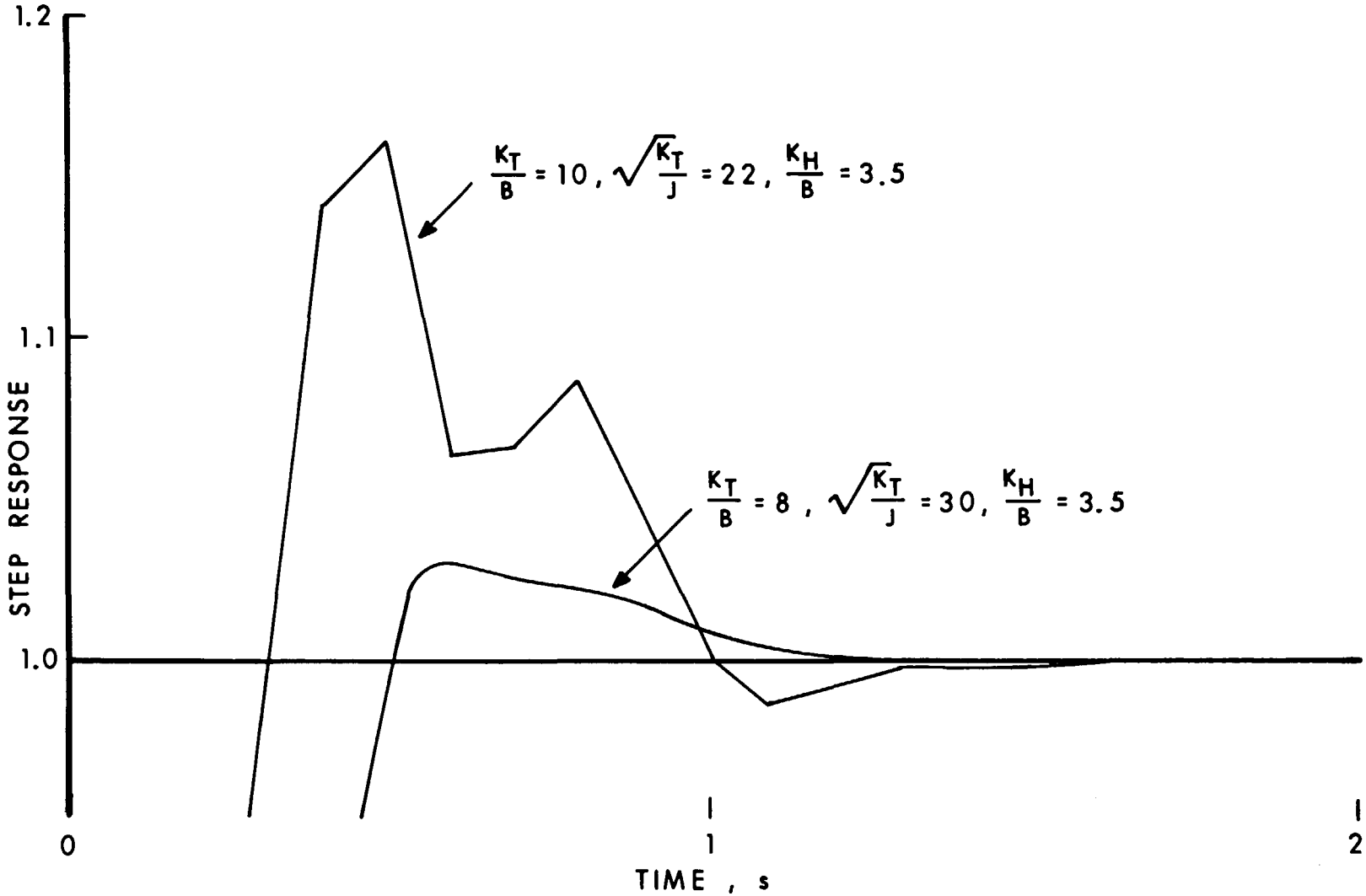

Figure 4. Closed Loop Response to a Step Input

TABLE II. List of Conditions for ITAE

K_H/B	K_T/B	$\sqrt{K_T/J}$	ITAE
3.0	10	15	.5093
3.0	10	22	.3247
3.0	10	30	.3140
3.0	10	40	∞
2.5	10	22	.4006
3.5	10	22	.3306
2.5	10	30	.3910
3.5	10	30	.2782
3.0	8	22	.3207
3.0	12	22	.4574
3.0	8	30	.2327
3.0	12	30	.4037
3.5	8	22	.5826
3.5	8	30	.1781
4.0	8	30	.2243
3.5	7	30	.2611
3.5	9	30	.2222
3.5	8	35	.1780

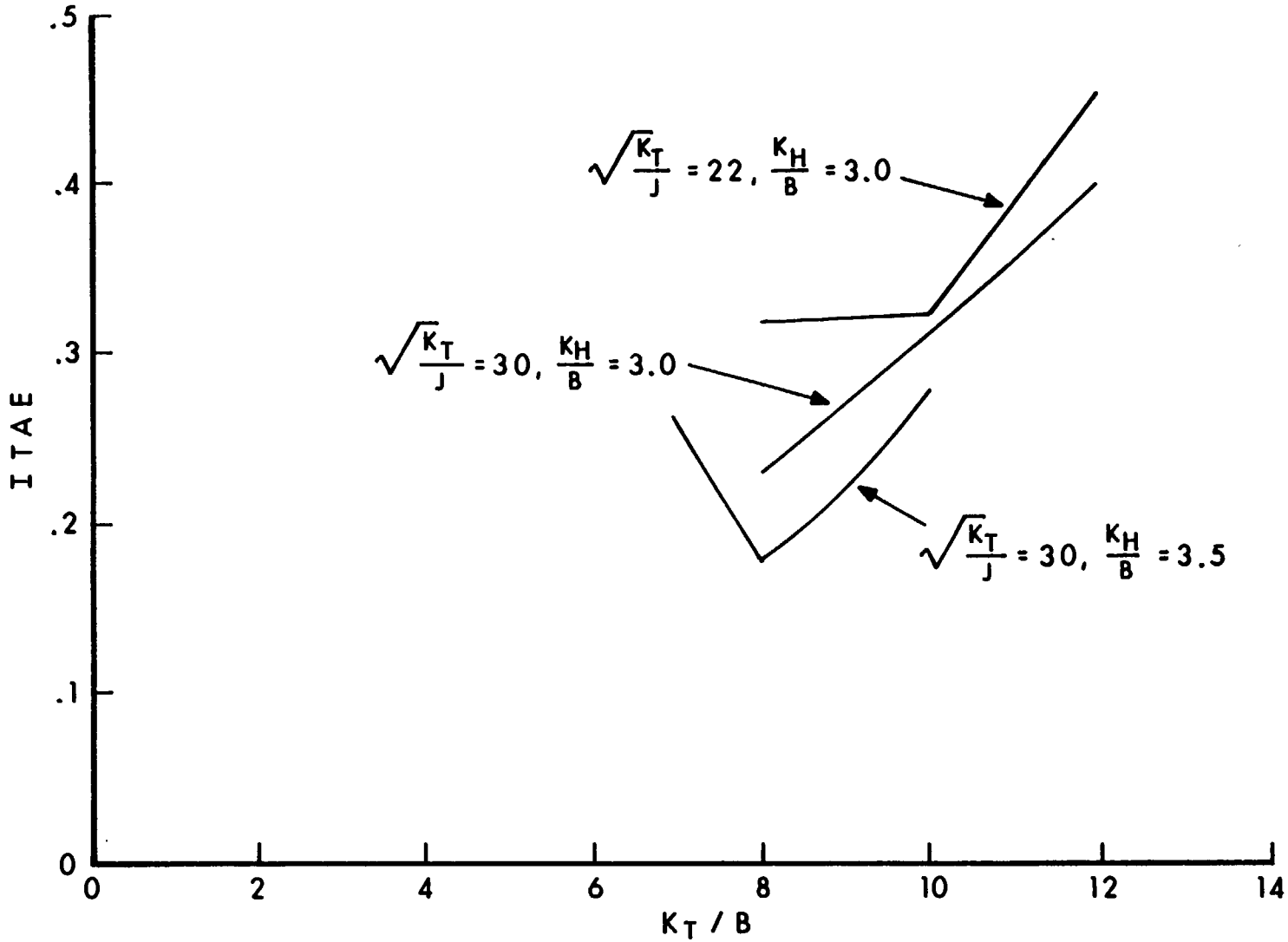

Figure 5. ITAE

drawn to help motivate this understanding even though the graphs are not to exact scale.

Figure 6(a) shows the root locus for a system with infinite stiffness. The pole at the origin is a free integration unaffected by anything we do. The pole and zero at -6.6 and +6.6 are the Padé approximation of a man assumed to be independent of tripod parameters. The pole at -25 is determined by the damping B. This plot shows that the locus near the origin is not going to be affected much by the value of B as long as it is greater than ten. The human in the loop will tend to adjust his gain until the closed loop root nearest the origin is near the dashed line indicating a damping ratio of 0.7. In general, the system response is improved if this root can be moved further away from the origin but still near the dashed line and of course high gain is desirable.

Figure 6(b) shows the locus of roots for a system with finite stiffness. An open loop zero is located at $-K_T/B$ and a pair of open loop poles are located at $-K_T/2B \pm \sqrt{\left(\frac{K_T}{2B}\right)^2 - \frac{K_T}{J}}$. For the condition shown here, K_T has been reduced just enough to make the pair of open loop poles at $-K_T/2B$ become imaginary; i.e., K_T is slightly less than $(2B)^2/J$. If $K_T > (2B)^2/J$, this pair of open loop poles would be real. The closed loop root near the origin will still be near the intersection with the dashed line and, therefore, it will not be affected significantly by small changes in K_T or B.

Figure 6(c) shows what happens after K_T has been reduced even more. The segment of locus crossing the imaginary axis (the stability limit) is now controlled by the open loop poles located at $-K_T/2B \pm j\sqrt{K_T/J}$ (approximate for reasonably large values of $\sqrt{K_T/J}$, say greater than 15). The closed loop root nearest the origin and along the dashed line is influenced by the location of the zero at $-K_T/B$. Now we can really affect the system performance by careful choice of these parameters. The plot in Figure 6(c) is getting near optimum because the intersection of the locus with the dashed line is able to move further away from the origin. In fact since a human can alter his gain somewhat, the actual operating point might be anywhere in the region of near tangency.

Figure 7 shows the root locus for the so-called ITAE optimum design. By increasing B the zero at $-K_T/B$ was moved closer to the origin and the locus "circle" became smaller, causing the system to be slightly more damped than the system in Figure 6(c). The closed loop root determined by the ITAE had $K_H/B = 3.5$. This point would fall about halfway between the closed loop roots shown. This system has good damping and good frequency response.

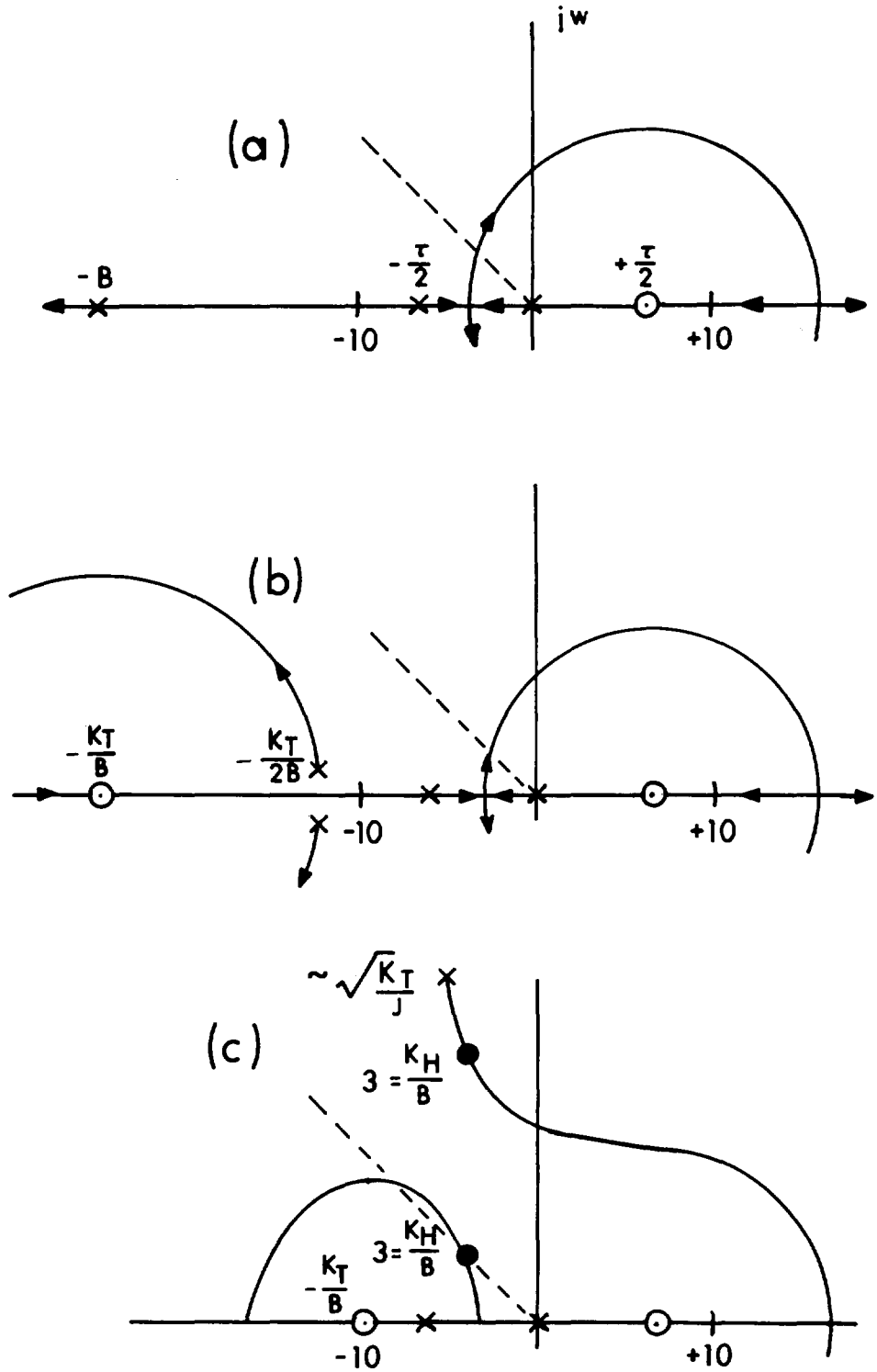

Figure 6. Root Locus Plots

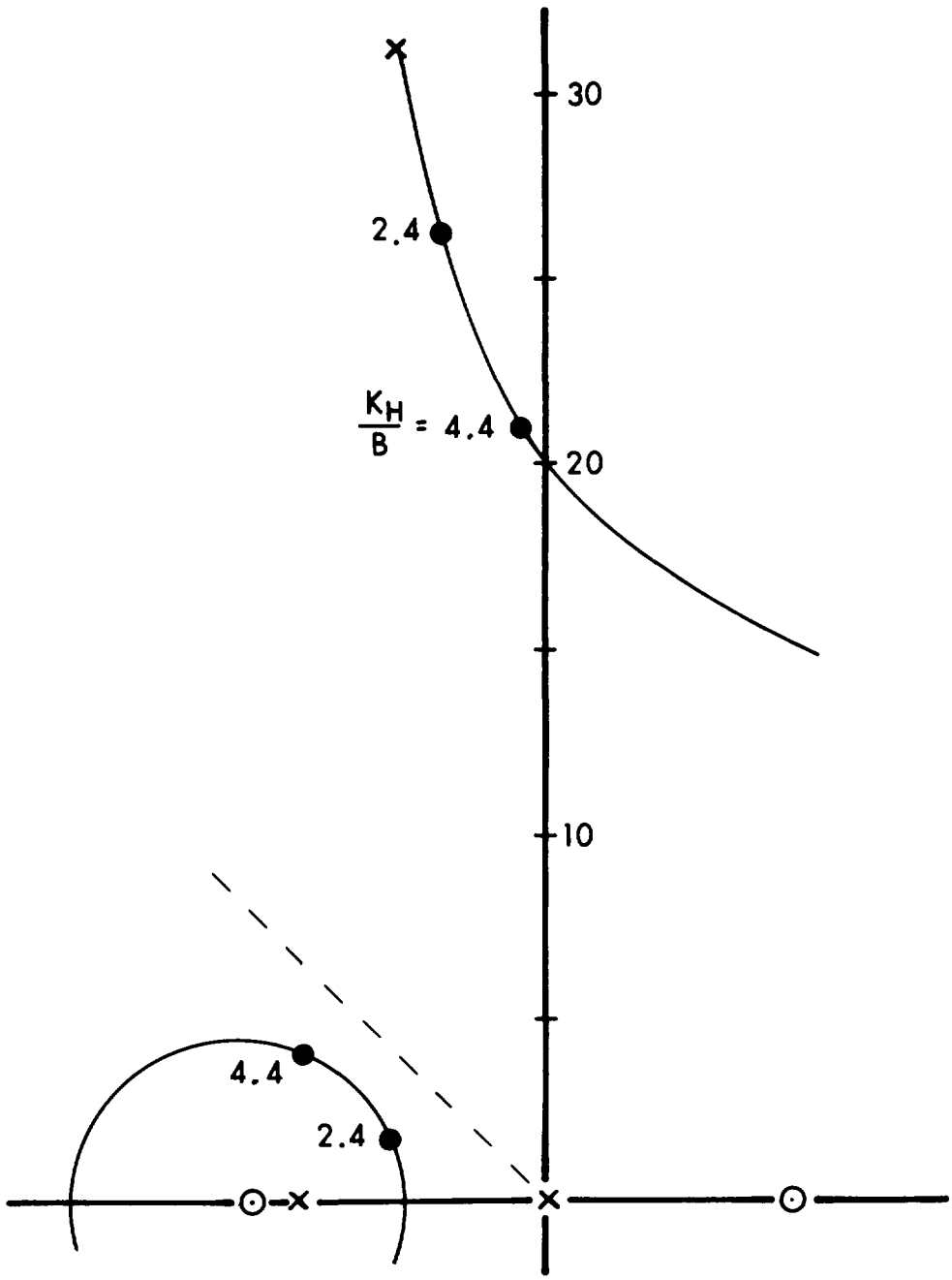

Figure 7. Root Locus of ITAE Optimum System

VII. SIMULATION

The simulation task attempted to validate the transfer function assumed for a human operator and to verify the trends found in the analyses. The effort consisted of developing an analog computer simulation of the tripod dynamics, writing a hybrid program to operate the analog and analyze the results, and interfacing a strain gage type force controller with the analog computer. Figure 8 shows the physical layout and the essential part of the analog circuit.

The experimental scheme required a subject to observe an error signal on a CRT. He attempted to reduce the error, i.e., return a dot to the center of the display, by applying a force to the strain gage control stick. The gage output signal entered the analog computer as a torque to drive the tripod. The tripod output angle, θ, was subtracted from the reference (filtered white noise source) and presented on the CRT.

The reference task was selected to meet two criteria. First, the task must not be predictable by the subject as a simple sine wave would be. Second, it must distribute the tracking energy evenly over the frequencies of interest so that the transfer function could be calculated. These criteria were met by using a gaussian random variable for the target acceleration. A new value was introduced every time step (mean 0.0, standard deviation 0.1). This value was passed through a second order filter to keep the energy requirement for input torque constant across the frequencies of interest. It was also necessary to reduce the low frequency drift to prevent overloading the filter integrator as shown in Figure 8. The filter transfer function then became $1/S(S + 1)$.

The data analysis was developed to calculate the human gain and phase lag every radian per second from zero to ten. The desired resolution of one radian per second determined that there be approximately one minute of continuous data to sample ten cycles. The maximum frequency of ten radians per second required that there be at least twenty samples per second to prevent aliasing, i.e., about ten times the frequency. The Fast Fourier Transform subroutine (FFT) required 2^N samples. With N = 9 there are 1024 samples equivalent to 51 seconds of data at 20 samples per second. This sample size gives 90 percent confidence of accuracy within 25 percent when there are ten frequency bands of interest. Therefore, each trial on the computer consisted of a 51-second data run plus a two-second warmup period to achieve steady state. Every time step (0.05 seconds) the error and the torque were A/D converted and stored and a new Gaussian sample was drawn and delivered, i.e., D/A converted.

The FFT subroutine was called to process both the error and torque data. In general the ratio of the output (torque) to input (error) will

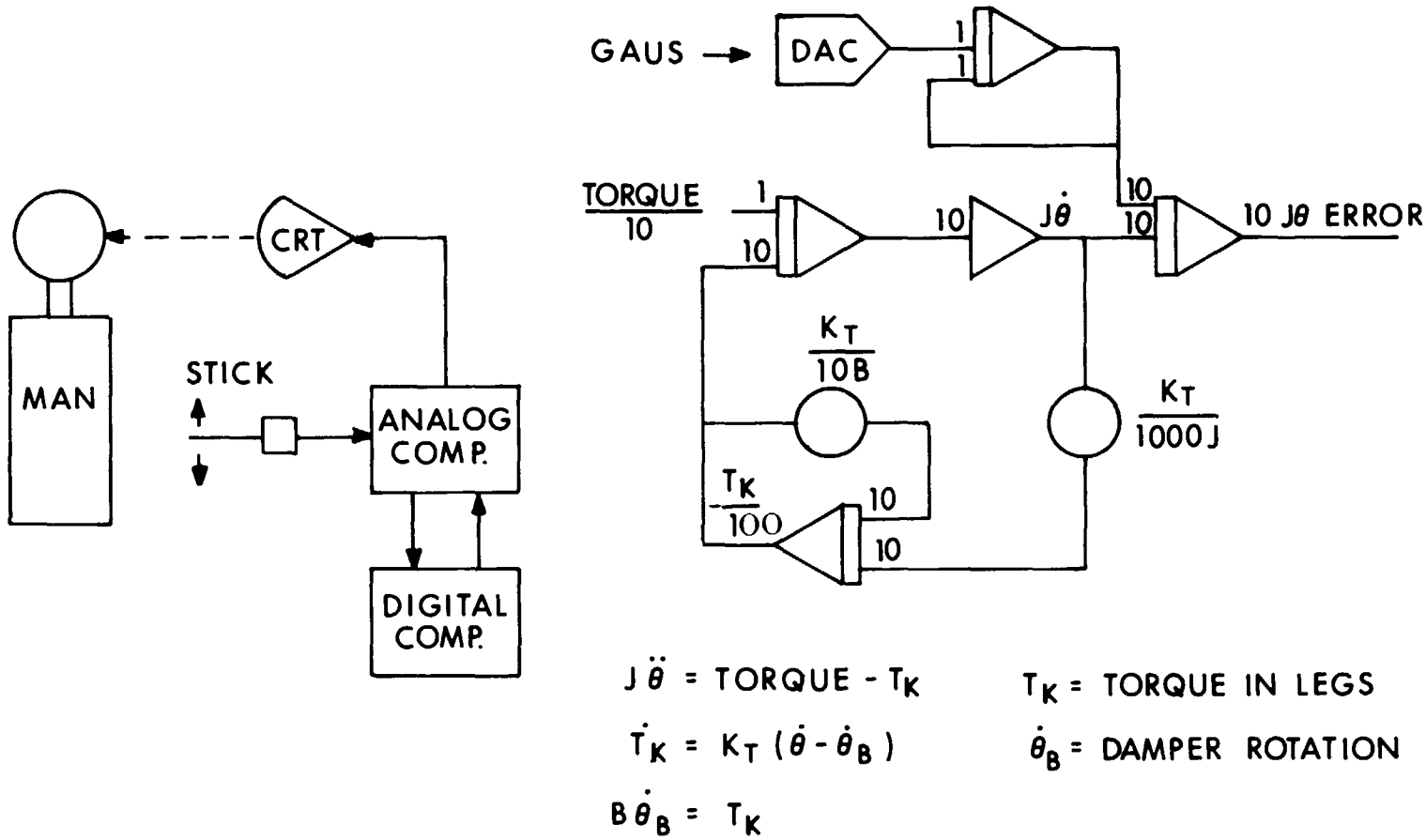

Figure 8. Simulation Scheme

yield the gain and phase as a function of frequency from which the transfer function can be constructed. In practice it was necessary to combine the vector pairs from eight frequency bands to obtain a one radian per second band. It was also necessary to rotate the vector pairs to a common reference (zero) to avoid going past 360° when calculating phase. The rotation was performed first, then the vector addition, then the division. The remaining vector contains the gain and phase. More averaging was achieved by running two repetitions for each of two subjects on each test condition. The averaged results for the four tests of each condition are presented in Figures 9 and 10.

The test conditions were chosen to give a wide variation in parameters based on the prior analysis and also evaluate some specific near optimum designs. The four-test condition had parameter values as shown below:

Condition	J	B	K_T	K_T/B	$\sqrt{K_T/J}$
I	1	50	200	4	14
II	1	50	500	10	22
III	1	50	∞	∞	∞
IV	1	120	1000	8	31

These tests should be considered like a pilot study. The test conditions were not properly counterbalanced to account for learning and there should have been a larger sample of subjects and repetitions before making any judgments about differences between test conditions. For example, the RMS tracking error was recorded during the tests but there was no significant difference between conditions. In fact, they were all about the same.

On the other hand, the plotted results on Figures 9 and 10 seem to validate the assumed human transfer function. The gain tends to be constant with frequency, i.e., within the 90 percent band of 2 db except for the last couple of frequency bands where the measurement energy might be too low.

The phase tends to fall off linearly with frequency. Actually, the phase follows the Padé approximation, shown by a dashed line, more closely than a pure delay which would have slope of -0.3 all the way. Another observation is that the assumed transfer function is a better fit for the test conditions with stiffer legs, i.e., K_T = 500, 1000, and ∞.

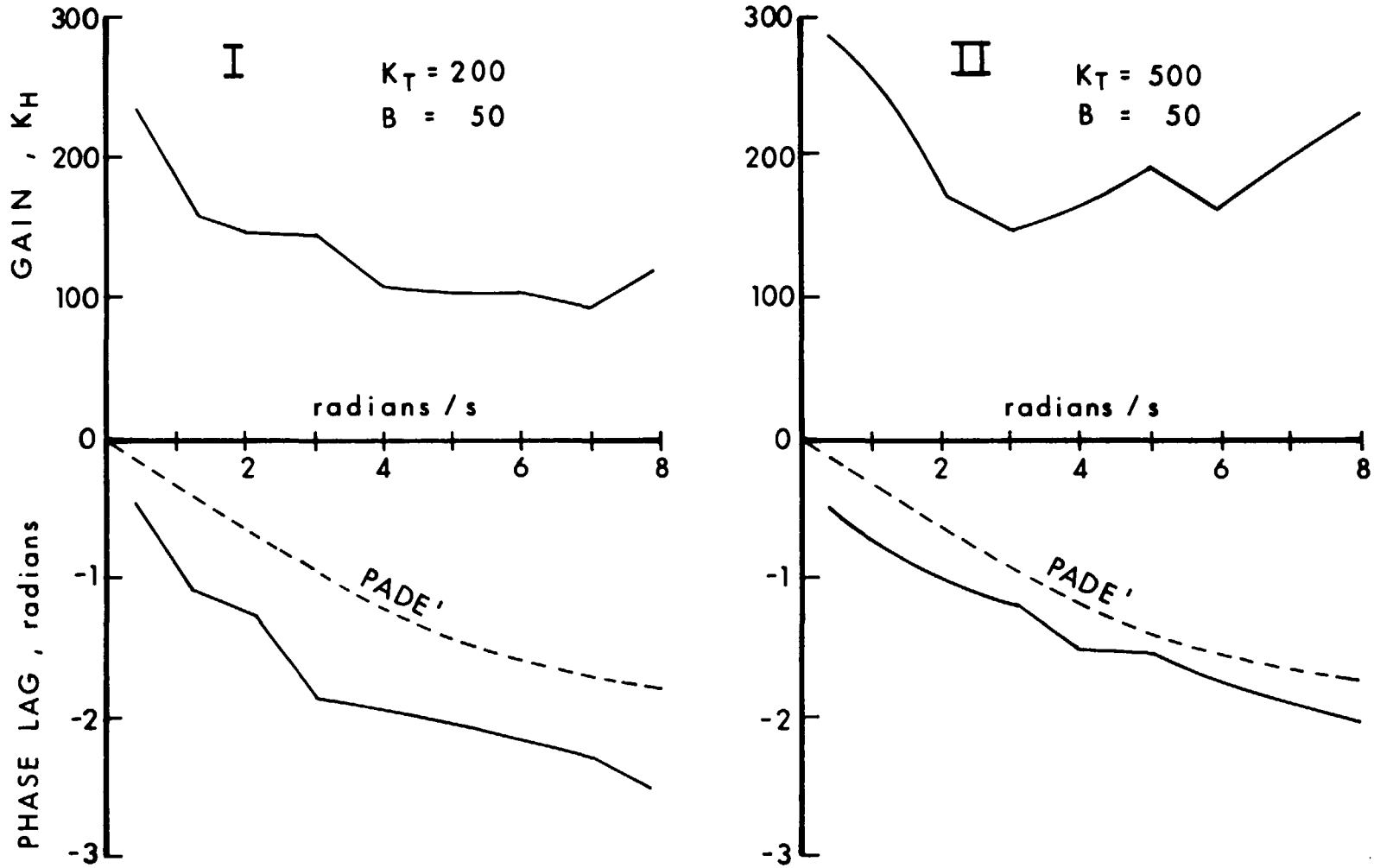

Figure 9. Gain and Phase Results of Simulation

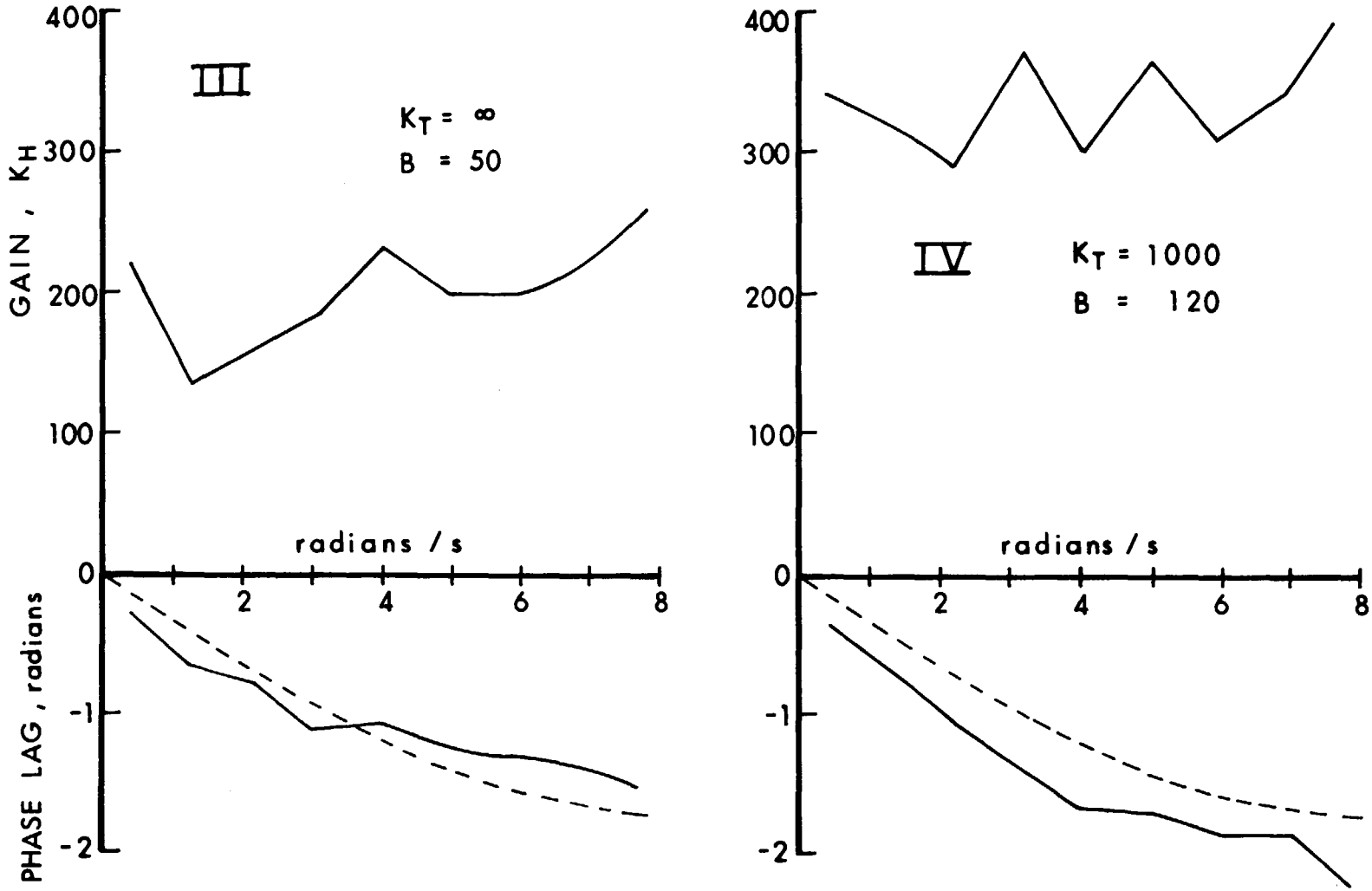

Figure 10. Gain and Phase Results of Simulation

VIII. DISCUSSION

Looking back over what has been done, I conclude that there is merit to the analysis of this control problem. The exact human transfer function is probably very similar to the one used in these analyses. The optimum parameter values are probably within the range indicated here, i.e., K_T/B between 8 and 14 and $\sqrt{K_T/J}$ equal to 30 or more. Moreover, it is possible to analyze such a problem, then confirm the results by simulation. Eventually these results should be supported by field experiments with hardware.

The area deserves more attention than it has received. There are any number of applications in addition to the military pointing task which inspired the current effort. The motion picture tripod is the most similar task but there are other tasks such as remote manipulation of a mass through mechanical linkage. This problem is a little different because the compliance is between the point of application of torque and the load rather than between the load and ground. Where should the viscous damping be introduced to stabilize this loop?

There are many things to do to continue the work started here. Some of them would improve the quality of results. Some of them would explore the simplifying assumptions made in the introduction. Others would expand the generality of the results.

a. The torque input device could be built to simulate a specific piece of hardware so that there could be field test data available for comparison. The actual torques and visual angles could be duplicated in the simulation. The reference task would need to be duplicated as well.

b. Once a good experimental setup has been established there should be more data and a more systematic experimental procedure should be followed.

c. The results should be expanded to include other forcing functions. Will the transfer function and the optimum design change much if the task is changed from white noise to step functions or to low frequency sine waves?

d. Other methods of introducing torque could be considered, e.g., two hands as with a steering wheel and twisting as when removing a jar lid.

e. The limits of linearity of the human transfer function could be defined both with respect to visual threshold and maximum torque.

f. Coulomb friction should be evaluated. It is expensive to minimize coulomb friction in a device so we should know just how much can be tolerated when there is a given level of viscous friction.

A human operator is very adaptable and he can usually manage to get by with a less than optimum tracking device. But a near optimal design will require less training; it will be easier to use; and it will give better performance when it really counts. Pursuing the research described above will help achieve better designs and perhaps even save money by preventing over design when it does not help.

ACKNOWLEDGEMENT

The work reported on here was done by the author while on long term training at the Massachusetts Institute of Technology Center for Advanced Engineering Study. Professor Henry M. Paynter provided guidance and encouragement throughout the duration of this effort.

No. of Copies	Organization
12	Commander Defense Documentation Center ATTN: DDC-TCA Cameron Station Alexandria, VA 22314
1	Commander US Army Materiel Development and Readiness Command ATTN: DRCDMA-ST 5001 Eisenhower Avenue Alexandria, VA 22333
1	Commander US Army Aviation Systems Command ATTN: DRSAV-E 12th and Spruce Streets St. Louis, MO 63166
1	Director US Army Air Mobility Research and Development Laboratory Ames Research Center Moffett Field, CA 94035
2	Commander US Army Electronics Command ATTN: DRSEL-RD DRSEL-CT-L-A, M. Mirachi Fort Monmouth, NJ 07703
2	Commander US Army Missile Command ATTN: DRSMI-R DRXHE-MI, J. Chaikin Redstone Arsenal, AL 35809
1	Project Manager DRAGON US Army Missile Command Redstone Arsenal, AL 35809
1	Project Manager Precision Laser Designators US Army Missile Command Redstone Arsenal, AL 35809
1	Project Manager TOW US Army Missile Command Redstone Arsenal, AL 35809
1	Commander US Army Tank Automotive Development Command ATTN: DRDTA-RWL Warren, MI 48090
2	Commander US Army Mobility Equipment Research & Development Command ATTN: Tech Docu Cen, Bldg 315 DRSME-RZT Fort Belvoir, VA 22060
1	Commander US Army Armament Command Rock Island, IL 61202
2	Commander US Army Picatinny Arsenal ATTN: SARPA-AD-D-R, Arnold Novak SARPA-AD-D, Lewis Cole Dover, NJ 07801
1	Commander US Army Watervliet Arsenal ATTN: SARWV-RDD-SE, Malcolm Dale Watervliet, NY 12189
1	Commander US Army Harry Diamond Labs ATTN: DRXDO-TI 2800 Powder Mill Road Adelphi, MD 20783
1	Director US Army TRADOC Systems Analysis Activity ATTN: ATAA-SA White Sands Missile Range, NM 88002

No. of Copies	Organization
1	Hughes Aircraft Company ATTN: Warren Smith Culver City, CA 90230
1	Massachusetts Institute of Technology 3-264 ATTN: Prof Henry M. Paynter Cambridge, MA 02139

No. of Copies	Organization
	Aberdeen Proving Ground
	Marine Corps Ln Ofc Dir, USAMSAA Joseph Sperrazza Walter Clifford James W. Brown Dir, USAHEL John D. Weisz Gary L. Horley James P. Torre Cdr, TECOM DRXTE-HF, Mr. C. N. McCain